

DEVELOPMENT OF STANDARD FOR ABSOLUTE MASS FLOW MEASUREMENT TO BE USED WITH ANY TYPE OF COMMON GAS

Ahmed S. Hashad ⁽¹⁾, Heiko Dartsch ⁽²⁾, Hans-Peter Harmann ⁽³⁾...

^{(1), (2), (3)} AST Advanced Space Technologies GmbH, Marie-Curie Strasse 16-18, 27711 Osterholz-Scharmbeck, Germany,

⁽¹⁾Email: ahmed.hashad@ast-space.com

⁽²⁾Email: dartsch@ast-space.com

⁽³⁾Email: harmann@ast-space.com

KEYWORDS: Mass flow rate measurement, Flow controllers, Thrusters, Electric propulsion

ABSTRACT:

The precision of propellant flow regulation in electric propulsion systems for space applications is crucial due to the limited propellant budgets of spacecraft. However, conventional industrial mass flow meters, typically calibrated using nitrogen or air, pose challenges when alternative gases like Xenon are used. Conversion factors used to adjust readings are often based on theoretical principles rather than real-world measurements, leading to measurement errors, especially with costly gases like Xenon. Such errors can be significant, impacting missions like Mars-Sample Return (MSR) requiring large quantities of Xenon.

To address this, an affordable in-house calibration setup, Gravimetric Mass Flow rate (**GMF**), has been developed, ensuring precise control of pressures, temperatures, and flow conditions. This paper details the implementation of this setup, addressing challenges and presenting a comprehensive error sources. Validation against commercially calibrated mass flowmeters shows high accuracy of the implemented test procedure, below 0.05%, with any commonly used gas for electric propulsion, making it versatile for various applications.

1. INTRODUCTION

In recent years, the demand for more capable and reliable satellites has intensified, driven by the growing need for telecommunications, Earth observation, navigation, and scientific exploration. Electric propulsion [1]–[4] systems offer a promising solution to meet these demands, characterized by their high specific impulse and efficiency compared to traditional chemical propulsion systems. However, their successful deployment hinges on the accurate determination of mass flow rates throughout the mission lifecycle.

The importance of precise mass flow rate measurement cannot be overstated. It directly influences key aspects of satellite operation, including orbit manoeuvring, station-keeping, and attitude control. Variations in mass flow rates can significantly impact the satellite's trajectory, fuel

consumption, and overall mission duration. Moreover, deviations from the intended flow rate can compromise the system's stability and performance, leading to suboptimal operation or mission failure.

Industrial mass flow meters are typically calibrated with nitrogen gas. When using a different gas, readings are adjusted using a flow-dependent conversion factor. However, these factors can vary between different types of mass flow meters and are often derived from theory rather than verified by real measurements, particularly for exotic gases like Xenon. Consequently, using such gases can result in measurement errors of a few percent.

2. GENERAL APPROACH

In the realm of fluid dynamics and engineering, the concept of mass flow rate stands as a fundamental parameter governing the movement of fluids through a system. Mass flow rate [5]–[7], denoted by the symbol \dot{m} , represents the change in mass over time is particularly useful for situations where the mass of a gas flowing through a system changes over a specific duration as in Eq. 1.

$$\dot{m} = \frac{m}{t} \quad \text{Eq. 1}$$

where m is the true mass of the gas transferred during the measurement, and t is the time duration of the measurement.

This approach is feasible if:

- the rate of change in flow rate is small compared to the response time of the measurement device under tests and the temporal resolution of the flow measurement so that time integration is possible
- the amount of gas inside of the test setup which is not accessed directly by mass measurement (e.g., gas contained in the pipework) has to be the same at the start and at end of the measurement.

Besides a precise measurement of the mass of gas consumed, the main design objective of the calibration setup is therefore to ensure the same conditions regarding pressures and temperature, stability of the gas density during the measurement, at the beginning and end of the test.

3. SETUP DESIGN

4. CALIBRATION SEQUENCE

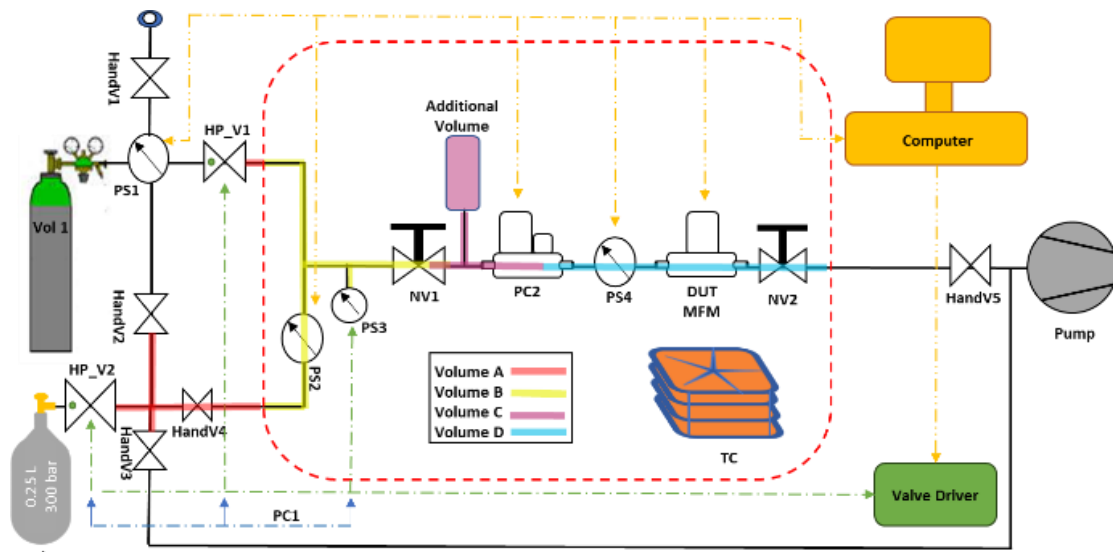


Figure 1. Schematic drawing of the GMF.

Components outlined by the dashed red line in Figure 1 are inside a temperature controlled environment. The inner temperature of the box is stabilized with $\pm 0.1^\circ\text{C}$ by an air heater. This also keeps the pressure sensors, well as the needle valves used as adjustable flow resistors at a constant temperature.

Calibration setup itself includes two gas containers, denoted as **Vol 1** and **Vol 2** in Figure 1. While **Vol 2** contains the gas which its mass is measured before and after the measurement. **Vol 1** is also used to fill the volume **Vol 2** with gas before the measurement via the hand valve **HandV2** while the hand valve **HandV3** allows for prior evacuation.

Before the start of the measurement itself, the whole setup is operated from the gas container **Vol 1** stable equilibrium flow conditions are established. The solenoid valves **HP_V1** and **HP_V2** facilitate seamless gas supply switching at the start of measurements, handing over to the gas supply **Vol 2**. Both valves, along with pressure sensor **PS3**, form a pressure regulator that maintains pressure by briefly opening when it falls below a threshold. First pressure controller (**PC1**) regulate the valves based on **PS3** readings and controlling pressure from 50 bar inlet to 5 bar with ± 0.050 mbar fluctuation.

Pressure ripple generated is negligible due to synchronization with measurement time. **PS2** monitors inlet pressure. Needle Valve (**NV1**) and **Additional Volume** dampen pressure ripple, and commercial pressure controller **PC2** practically eliminates fluctuations lower than ± 2 mbar.

1. • Evacuate **Vol 2**.
2. • Fill **Vol 2** with the supplied gas by 20 to 50 bar.
3. • Disconnect and Weigh **Vol 2** including **HP_V2** (after filling).
4. • Reconnect **Vol 2** to the setup and evacuate **Volume A**.
5. • Test the leakage and open **HandV4**
6. • Identify the measurement time and **MFM** vale need to be calibrated using **NV2**
6. • Start the pressure controllers **PC1** using **Vol 1** untill stability.
7. • Start the measurement by switching **PC1** using **Vol 2**.
8. • Pressure, temperature and flow values are recorded during the measurement time.
9. • Disconnect and Weigh again **Vol 2** including **HP_V2** (after measurement stop).
10. • Calculate the absolute mass flow rate (**MFR**).

5. GMF UNCERTAINTY SOURCES

For an assessment of the calibration accuracy the following sources of uncertainty, as shown in Figure 2, have to be taken into account.

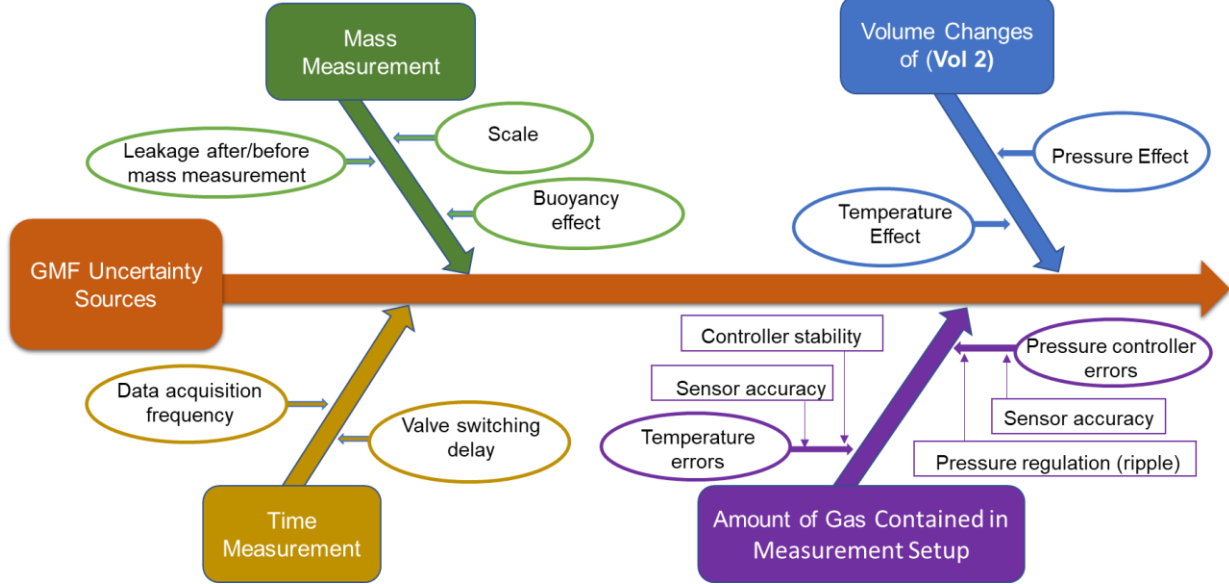


Figure 2. Error scheme of GMF measurement system.

Together with the time related and mass measurement related error contributions presented above the overall relative error of the mass flow measurement can now be expressed as in Eq. 2 since the individual contributions are independent of each other.

$$\frac{\Delta \dot{m}}{\dot{m}} = \sqrt{\left(\frac{\Delta \dot{m}}{\dot{m}}\right)_{switching}^2 + \left(\frac{\Delta \dot{m}}{\dot{m}}\right)_{sampling}^2 + \frac{1}{t^2} \cdot \left[\left(\frac{\Delta m}{m}\right)_{scale}^2 + \left(\frac{\Delta m}{m}\right)_T^2 + \left(\frac{\Delta m}{m}\right)_p^2 \right]} \quad \text{Eq. 2}$$

$\Delta \dot{m}$ is the uncertainty of the mass flow rate, uncertainty contribution on the true mass according of the weighing scale is denoted by $(\Delta m)_{scale}$, $(\Delta m)_T$ is the uncertainty of true mass as a function of temperature changes, and $(\Delta m)_p$ is the uncertainty of true mass as a function of pressure changes.

Herewith, relative error is inversely proportional to the measurement time t .

5.1. Time Measurement Uncertainty

Measurement is started by detecting the pressure level crossing with the sensor **PS3** and opening the valve **HP_V2**. The end of measurement is also defined by detecting the same type of level crossing at a later point in time. A worst-case limit for the time uncertainty Δt_{valve} of 10 ms for the overall valve operations is stated above and the error contribution calculated by means of Eq. 3.

$$\Delta \dot{m} = \frac{m}{t} * \frac{\Delta t_{valve}}{t} = \dot{m} * \frac{10 \text{ ms}}{t} \quad \text{Eq. 3}$$

In term of the relative flow error the contribution calculate using Eq. 4.

$$\left(\frac{\Delta \dot{m}}{\dot{m}}\right)_{switching} = \frac{10 \text{ ms}}{t} \quad \text{Eq. 4}$$

The average of the reading of device under test is

integrated over the measurement time. The worst-case uncertainty contribution is given by the time difference between two measurements.

Uncertainty in average mass flow expressed as relative flow error using the measurement time and the acquisition frequency $f_{acquisition}$ as in Eq. 5

$$\left(\frac{\Delta \dot{m}}{\dot{m}}\right)_{sampling} = \frac{1}{t * f_{acquisition}} \quad \text{Eq. 5}$$

The acquisition frequency depends on the instrument to be calibrated.

5.2. Mass and Volume Measurement Uncertainty

These include uncertainties associated with direct mass measurements by using weighing scale, as well as uncertainties linked to the precise determination of the gas quantity contained within the experimental setup e.g. (Buoyancy effect and system leakage).

- Weighing scale used for the mass measurement of the volume **Vol 2** before and after the calibration has repeatability of 1 mg and linearity of ± 2 mg. However, since the change in mass to be measured is typically in the order of less than 10 g the corresponding (worst-case) contribution of the scale to the error in mass is regarded as being the stated repeatability as shown in Eq. 6

$$(\Delta m)_{scale} = 1 \text{ mg} \quad \text{Eq. 6}$$

In terms of the relative flow error the contribution of the mass measurement on the uncertainty is calculated by means of Eq. 7.

$$\left(\frac{\Delta \dot{m}}{\dot{m}}\right)_{scale} = \frac{(\Delta m)_{scale}}{t * \dot{m}} = \frac{1 \text{ mg}}{t * \dot{m}} \quad \text{Eq. 7}$$

- The volume **Vol 2** is constructed from stainless steel wrapped with carbon fibre to optimize weight. Consequently, fluctuations in the pressure within **Vol 2** occur between measurements before and after calibration, causes the container to shrink, introducing an additional error during mass measurements under atmospheric pressure due to buoyancy effect. To address this, the density of air is considered to be slightly above 1 mg/cm³. Therefore, change in volume of the container by 1 cm³ roughly corresponds to an error in mass measurement of 1 mg. However, as **Vol 2** has a nearly cylindrical shape, measurements of its outer diameter and length prior to each mass measurement allow for the correction of buoyancy effects to a significant extent, rendering the remaining impact negligible.

Regarding the Buoyancy effect the change in air density with temperature and pressure also has to be taken into account. Here the correction has to be applied in terms of the air volume displaced by the whole container including the valve and pipework. Since the change in air density is rather small over the temperature and pressure range to consider and the remaining error after applying the corresponding correction is related only to the uncertainty in knowledge of the exact volume, its contribution to the overall error is small compared to other error sources and can therefore be neglected.

- An internal leakage of the valve HP_V2 could affect the mass measurement if a significant amount of gas is lost before after/before the measurement is taken. For the type of valve used the (He-) leakage is better than 1e⁻⁶ scm³/s. Even for relatively heavy gases like Xenon with a density of about 6 mg/cm³ this translates into a loss of less than 0.1 µg/second. This means that for any reasonable time between measurements the error contribution from valve leakage can be neglected.

5.3. Gas Contained in Measurement Setup

The used method for calibration can only be exact if the amount of gas which is taken from the container **Vol 2** and the amount of gas which is passed the instrument to be calibrated during the time of measurement are equal. This is achieved by starting and stopping the measurement under at the same pressure and temperature conditions, constant gas density.

The amount of gas inside of the setup is defined by the volume of the setup and the density of the gas. GMF setup was analysed and separated into four temperature and pressure regimes as shown in Figure 1 (Volume A, B, C & D). Since the setup temperature is always at least at room temperature (here defined as 23°C ±5°C) and the pressure

inside the setup (at the beginning and at the end of the measurement) is fairly small, in the order of 5 bar maximum, the gas density ρ is a linear function of the pressure and the (absolute) temperature, for all gases to be used for calibration like N₂, Krypton, Xenon. (Approximation of an ideal gas.)

Regarding the temperature error ΔT the contribution of the section (volume X) to the mass uncertainty by means Eq. 8.

$$(\Delta m)_{X,T} = V_X * p_X * \Delta T_X * \frac{\rho_0}{p_0 * T_0} \quad \text{Eq. 8}$$

where V_X is the volume of the section, p_X is section pressure and T₀ is (absolute) temperature of the section. ρ₀ is the gas density at the given reference pressure p₀ (e.g. 1 bar).

Also, pressure measurement or regulation Δp, the contribution of the section (volume X) to the mass uncertainty by means Eq. 9.

$$(\Delta m)_{X,p} = V_X * \Delta p_X * T_X * \frac{\rho_0}{p_0 * T_0} \quad \text{Eq. 9}$$

where T_X is the (nominal) temperature of the section.

As shown in Figure 1, the pressure in sections A and B are the same, while the temperature in sections B, C, and D are the same. Due to this correlation, the corresponding errors have to be added as worst-case absolute, while the other contributions are non-correlated and therefore are to be taken into account as sum of squares. For the temperature related error, the combined error calculated by means of Eq. 10.

$$\begin{aligned} (\Delta m)_T &= \sqrt{(\Delta m)_{A,T}^2 + [(\Delta m)_{B,T} + (\Delta m)_{C,T} + (\Delta m)_{D,T}]^2} \\ &= \frac{\rho_0}{p_0 * T_0} \\ &* \sqrt{(V_A * p_A * \Delta T_A)^2 + [(V_B * p_B + V_C * p_C + V_D * p_D) * \Delta T_{BCD}]^2} \end{aligned} \quad \text{Eq. 10}$$

For the pressure related error, the combined error calculated by means of Eq. 11.

$$\begin{aligned} (\Delta m)_p &= \sqrt{[(\Delta m)_{A,p} + (\Delta m)_{B,p}]^2 + (\Delta m)_{C,p}^2 + (\Delta m)_{D,p}^2} \\ &= \frac{\rho_0}{p_0 * T_0} \\ &* \sqrt{[(V_A * T_A + V_B * T_B) * \Delta p_{AB}]^2 + (V_C * T_C * \Delta p_C)^2 + (V_D * T_D * \Delta p_D)^2} \end{aligned} \quad \text{Eq. 11}$$

From Eq. 2, together with the time related and mass measurement related error contributions presented the overall relative error of the mass flow measurement can now be expressed as in Eq. 12

$$\begin{aligned} \frac{\Delta \dot{m}}{\dot{m}} &= \frac{1}{t} * \sqrt{(10 \text{ ms})^2 + \left(\frac{1}{f_{acquisition}}\right)^2 + \frac{1}{\dot{m}^2} * [(\Delta m)_{scale}^2 + (\Delta m)_T^2 + (\Delta m)_p^2]} \end{aligned} \quad \text{Eq. 12}$$

In the case of :

$$(10 \text{ ms})^2 + \left(\frac{1}{f_{acquisition}}\right)^2 \ll \frac{1}{\dot{m}^2} * [(\Delta m)_{scale}^2 + (\Delta m)_T^2 + (\Delta m)_p^2],$$

the relative error in flow rate resulting from the valve switching time and the acquisition frequency can be neglected. The relative uncertainty of the flow rate can be simplified by means of

$$\frac{\Delta \dot{m}}{\dot{m}} = \frac{1}{t * \dot{m}} * \sqrt{(\Delta m)_{scale}^2 + (\Delta m)_T^2 + (\Delta m)_p^2}$$

$$= \frac{1}{m} * \sqrt{(\Delta m)_{scale}^2 + (\Delta m)_T^2 + (\Delta m)_p^2}$$

Eq. 13

Hence, the relative mass flow calibration error is inversely proportional to the total mass transferred through the instrument to be calibrated.

6. VALIDATION RESULTS

Subsequent measurements were conducted employing (GMF) apparatus to evaluate the maximum error impacting flow rate measurements. These measurements aimed to empirically verify the computed accuracy of the GMF.

To validate the results, reference measurements were conducted using Nitrogen, as mass flow meters typically undergo calibration by their manufacturers using Nitrogen or air. It is noteworthy that the measurement principle of the GMF remains independent of the gas type utilized in the experiments.

6.1. Temperature Stability

Figure 3 illustrates the temperature stability of the GMF controlled setup during the flow measurement at different three measurement cycles. The standard uncertainty is about $\pm 0.2^\circ\text{C}$.

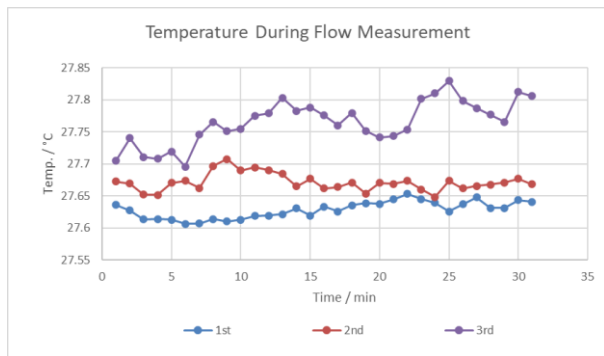


Figure 3. Temperature stability of GMF setup during Flow measurement.

6.2. Comparison Results

GMF was compared against calibrated 200 sccm commercial mass Flow Meter (**MFM**) using N₂ as gas supply. Three measurements were performed at different mass flow rate values (190 sccm, 120 sccm and 50 sccm).

The results are shown in Figure 4, Figure 5 and Figure 6 respectively.

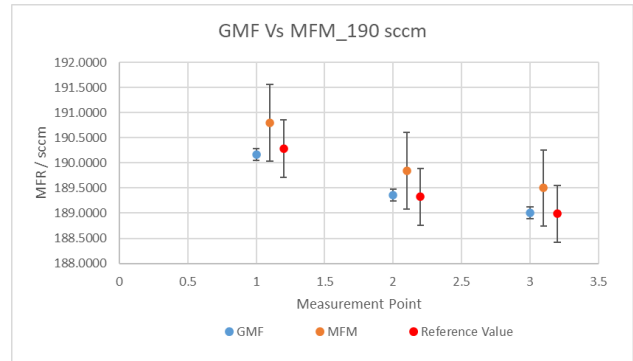


Figure 4. : Comparison of GMF against MFM using N₂ at 190 sccm.

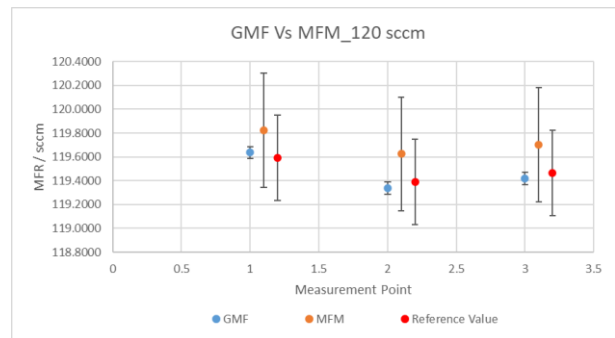


Figure 5. Comparison of GMF against MFM using N₂ at 120 sccm.

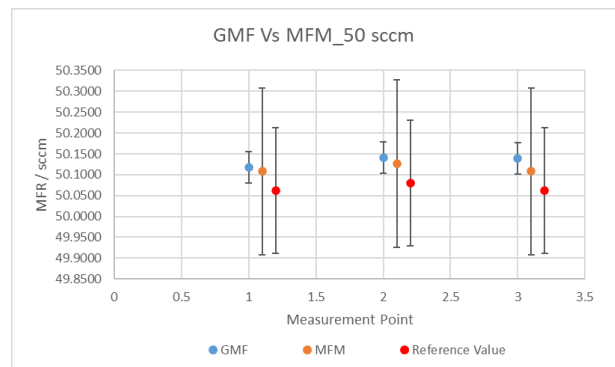


Figure 6. Comparison of GMF against MFM using N₂ at 50 sccm.

The results shows a full agreement of both standards with their accuracy at different mass flow rate values.

The reference values, red points, reflect the corrected values from the calibration certificate of the **MFM**.

All measurements are in line with the stated accuracy of the mass flow meter used for comparison.

The minimum error which can be achieved with this calibration setup is therefore determined by the amount of gas stored in the container **Vol 2** which can be used for calibration.

The nominal volume of the container **Vol 2** is 250 ml

(worst-case, w/o pipework and valve).

Assuming that the pressure in the container shall not exceed 50 bar for practical reasons (the container itself is rated for 300 bar) and the maximum pressure at start and end of calibration is 5 bar, the worst-case (minimum) mass available can be calculated from the difference in density for the specific type of gas where also the worst-case temperature difference ($23^{\circ}\text{C}\pm 5^{\circ}\text{C}$) can be taken into account.

Usable mass and resulting achievable calibration error for different gases is listed in Table 1.

Table 1. Usable mass for calibration and resulting achievable calibration error for different gases.

Gas	Usable Mass (g)	Achievable calibration error (%)
N₂	12.58	0.0225
He	1.75	0.0611
Ar	18.41	0.0212
Kr	42.02	0.0190
Xe	90.76	0.0138

7. CONCLUSION

Affordable setup was developed at AST to allow in-house calibration of flow measurement equipment with any common type of gas. This setup relied on quantifying the mass of gas depleted from a container during a defined period of time. This approach required ensuring that the same amount of gas was being used from the container and flowing through the device to be calibrated.

Error analysis also covered methods to ascertain calibration uncertainty concerning pressure and temperature stability. It was necessary to maintain the same amount of gas inside all other parts of the setup (e.g., pipe work, valves, etc.) at the start and the end of the calibration measurement. Achieving this required precise control of pressures and temperatures inside all parts of the setup. Additionally, stable flow conditions had to be established before the start of the calibration measurement process.

Solutions were found for the challenges mentioned above. Furthermore, the full error budget was presented in detail, showing that an accuracy of better than 0.05% could be achieved with any type of gases commonly used for electric propulsion.

Validation of the test system was conducted by comparing it to a commercially calibrated mass flow meter, employing nitrogen gas as the test medium. Ultimately, this flow calibration system was versatile and could be applied with a wide range of different gases.

8. REFERENCE

1. Jahn, R. G. & Choueiri, E. Y. (2003). Electric Propulsion. in *Encyclopedia of Physical Science and Technology* 125–141 (Elsevier, 2003). doi:10.1016/B0-12-227410-5/00201-5.
2. Brezina, A. J. & Thomas, S. K. (2013). Measurement of static and dynamic performance characteristics of electric propulsion systems. in *51st AIAA Aerospace Sciences Meeting including the New Horizons Forum and Aerospace Exposition 2013* (2013). doi:10.2514/6.2013-500.
3. Jahn, R. G. *ELECTRIC PROPULSION*.
4. Boyd, I. D. (2005). Numerical modeling of spacecraft electric propulsion thrusters. *Progress in Aerospace Sciences* vol. 41 669–687 Preprint at <https://doi.org/10.1016/j.paerosci.2006.01.001> (2005).
5. Sharipov, F. & Seleznev, V. (1998). Data on internal rarefied gas flows. *J Phys Chem Ref Data* **27**, 657–706.
6. Abdallah, A. *Fundamental Aspects of Rarefied Gas Dynamics and Hypersonic Flow*.
7. Lemmon, E. W. & Jacobsen, R. T. (2004). Viscosity and thermal conductivity equations for nitrogen, oxygen, argon, and air. *Int J Thermophys* **25**, 21–68.